

Microstructure and wear of some high-tensile brasses

A. WAHEED

Pakistan Institute of Nuclear Science and Technology, P.O. Nilore, Islamabad, Pakistan

N. RIDLEY

Manchester Materials Science Centre, Grosvenor Street, Manchester M1 7HS, UK

The relationship between microstructure, coefficient of friction and wear behaviour against mild steel has been examined for three commercially extruded high-tensile brasses, containing additions of manganese (~ 3 wt%) and silicon (~ 1 wt%). The alloys contained an approximately constant volume fraction of Mn_5Si_3 (6–7%) but the proportions of the α and β phases present were varied widely both by heat treatment and by changing the composition, particularly the aluminium content which lay in the range 0–3 wt%. A conventional pin-on-rotating-disc configuration with different loads and sliding speeds was used to determine the wear and the coefficient of friction. The effect of heat treatment on the wear behaviour of given alloys was complex, and depended on the volume fraction of the α and β phases, on their distribution in the microstructure, and on the ease with which the hard Mn_5Si_3 particles became detached from the phases in which they were located. The average coefficient of friction for the materials examined was 0.36 ± 0.02 and showed little variation with composition and microstructure, but it was clear that the experimental data was being influenced by detachment of Mn_5Si_3 particles. Results for the three alloys examined are presented and discussed.

1. Introduction

High-tensile brasses are $\alpha + \beta$ or β brasses which contain alloying additions such as aluminium, silicon, iron, manganese and tin. The additions strengthen the brasses by entering into solid solution, by forming intermetallic phases, by influencing the volume fraction of β -phase in the alloy, and by giving microstructural refinement. As well as high strength, the additions may confer good bearing properties and high wear resistance [1, 2]. In the case of alloys containing additions of manganese and silicon, particles of manganese silicide (Mn_5Si_3) are formed [3, 4]. These particles have a hexagonal crystal structure and high hardness, and give the alloy a high wear resistance [3]. These alloys find applications in the automobile industry, particularly in gear boxes, where a high resistance to wear is the chief requirement.

In the present work the relationship between microstructure, coefficient of friction and wear behaviour against mild steel has been examined for three commercial Mn–Si brasses. The alloys contained similar

volume fractions of manganese silicide phase (Mn_5Si_3), but the proportions of α and β phases have been varied by compositional changes and by heat treatment.

2. Experimental procedure

Three alloys coded as 326, SIB and E133 were supplied in the form of extruded bars by Mckechnie Metals Ltd, Walsall, UK. The compositions of these alloys are listed in Table I. Small specimens were cut from each bar and annealed in air over a temperature range of 200–800 °C in a resistance-heating furnace. This heat treatment was carried out to vary the volume fraction of α -phase as a function of temperature. Some specimens from each alloy were heated in the β -phase region (~ 550 °C) for 30 min followed by slow cooling (~ 20 °C h^{-1}) to room temperature. The object of the slow cooling was to obtain the maximum separation of α -phase in each alloy.

TABLE I Composition of alloys (wt %)

Alloy	Cu	Sn	Pb	Fe	Al	Mn	Ni	Sb	As	Si	Zn
326	61.84	0.9	0.53	0.25	3.24	3.02	0.3	0.03	0.006	0.72	Balance
SIB	59.67	0.07	0.14	0.18	1.62	3.30	0.02	0.005	0.006	1.06	Balance
E133	60.40	0.1	1.24	0.23	0.014	2.43	0.04	0.006	0.007	0.96	Balance

2.1. Metallography

For optical microscopic examination, specimens were metallographically polished following the standard procedure up to 0.25 μm diamond finish. They were etched in a solution of 1 g FeCl_3 and 20 ml concentrated HCl in 100 ml of water. Point counting was used to determine the volume fraction of different phases present in extruded and heat-treated alloys. Microanalysis was carried out for different phases using a Philips 505 scanning electron microscope (SEM) with an energy-dispersive X-ray detector.

2.2. Hardness, wear and friction testing

Vickers hardness tests were carried out for each extruded as well as heat-treated alloy using a 10 kg load. Microhardness for individual phases was determined using a Reichart microhardness tester with a 20 g load. Wear and friction tests were carried out against mild steel using the conventional pin-on-rotating-disc configuration. Different combinations of load and sliding speed were used for these tests. All tests were performed in air and in dry conditions without any lubricant. Tangential force was measured to determine the coefficient of friction by means of a transducer attached with the pin-on-disc apparatus. The output of the transducer was graphically plotted through a transducer converter and chart recorder.

3. Results

3.1. Microstructure of the extruded alloys

The microstructure of extruded alloys 326 and SIB in transverse and longitudinal directions is shown in Figs 1 and 2, respectively. They show light etching areas of α -phase which have a Widmannstätten morphology, a darker etching matrix of β -phase, and rod-shaped manganese silicide (Mn_5Si_3) particles with hexagonal cross-section. Preferential orientation of Mn_5Si_3 particles occurred during extrusion. The volume fractions of α and β -phases in alloy 326, as determined by point counting, were 9.6 and 85%, respectively, while the balance was Mn_5Si_3 . The volume fractions of α and β -phases in alloy SIB were 20 and 73%, respectively, with the balance being Mn_5Si_3 .

The microstructure of extruded alloy E133 (Fig. 3) was different as compared to alloys 326 and SIB. The matrix was of α -phase rather than β in this alloy. It consisted of nearly 81% α -phase and 13% β -phase, with the balance being manganese silicide particles.

3.2. Microstructure of the heat-treated alloys

Fig. 4 shows the variation of α -phase volume fraction as a function of temperature. In alloys 326 and SIB the α -phase vanished at 525 $^\circ\text{C}$, and above this temperature the microstructure consisted only of β -phase and the manganese silicide particles. In alloy E133 it appears that α -phase vanishes at about 820 $^\circ\text{C}$. However, in practice it was not possible to obtain a completely β structure for this alloy on quenching. The fastest cooling rate obtained was not rapid enough com-

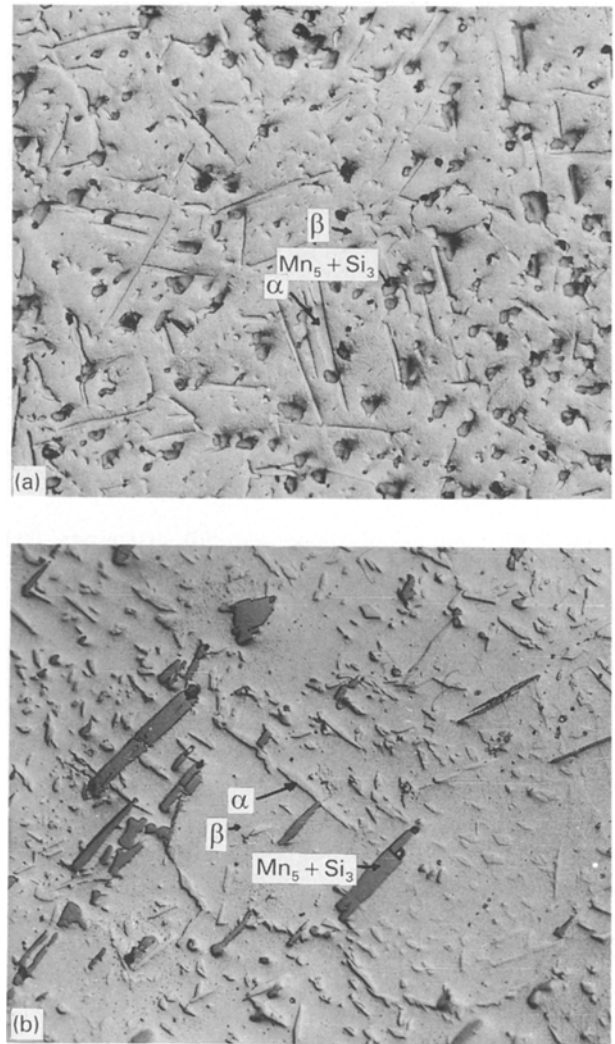


Figure 1 Microstructure of extruded alloy 326: (a) transverse, (b) longitudinal.

pletely to suppress the appearance of α -phase in this alloy. The maximum separation of α -phase was 22, 25 and 86% for alloys 326, SIB and E133, respectively.

3.3. Mechanical properties

3.3.1. Hardness

Table II shows the average Vickers Pyramid Number (VPN) for the extruded and furnace-cooled alloys. It is obvious from the table that alloy 326 is the hardest of the three, while alloy E133 is the softest. Table III shows the average microhardness for the individual phases in the alloys. In extruded alloy 326, the grain size of α -phase was not big enough to accurately measure the phase hardness.

3.3.2. Wear behaviour

Fig. 5 shows the comparison of wear behaviour for the extruded alloys at 0.16 m s^{-1} sliding speed. Weight loss during sliding was normalized against the cross-sectional area of the specimen and plotted as a function of applied stress. There was no significant difference in the wear of alloys 326 and SIB. Relatively large wear was observed for alloy E133, which was the softest of the three.

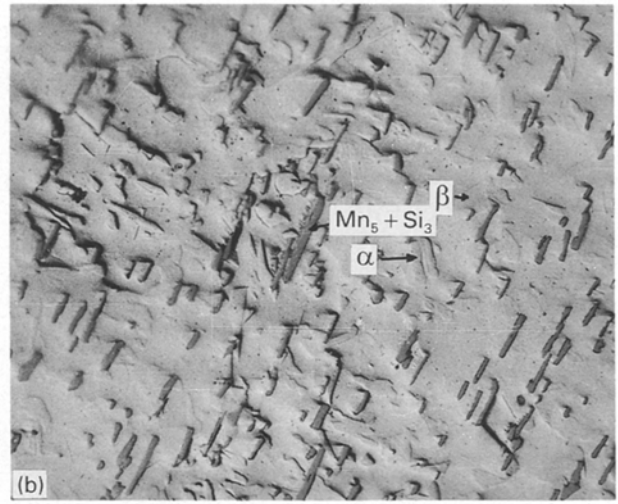
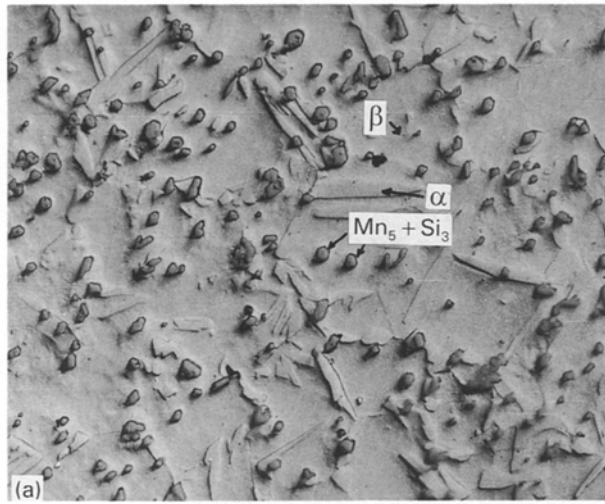


Figure 2 Microstructure of extruded alloy SIB: (a) transverse, (b) longitudinal.

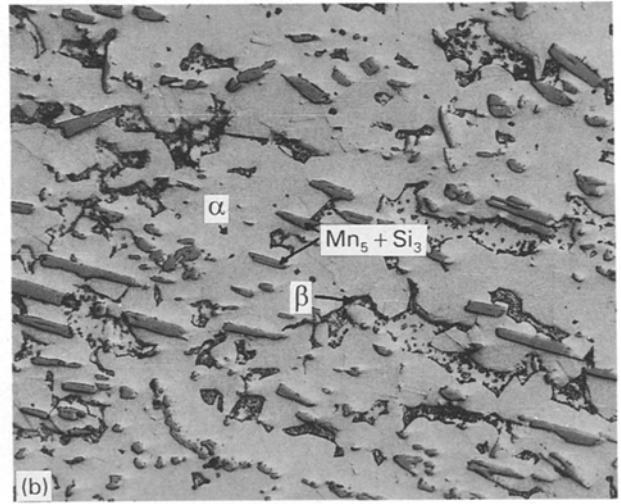
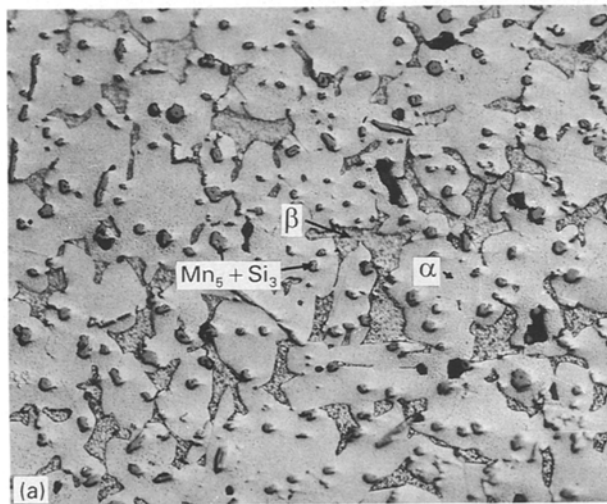


Figure 3 Microstructure of extruded alloy E133: (a) transverse, (b) longitudinal.

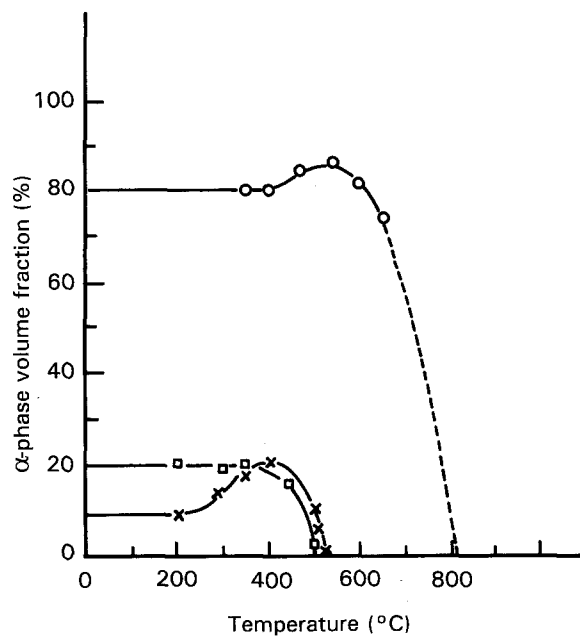


Figure 4 Variation in α -phase volume fraction as a function of temperature. ○, E133; □, SIB; ×, 326.

TABLE II Average hardness of extruded and annealed alloys at 10 kg load

Alloy code	Average hardness (VPN)	
	Extruded alloys	Annealed alloys
326	231	205
SIB	174	154
E133	106	90

TABLE III Average microhardness (VPN) of different phases in alloys at 20 g load

Alloy code	Extruded alloys		Annealed alloys	
	α -phase	β -phase	α -phase	β -phase
326	Not possible*	241	133	225
SIB	127	219	110	203
E133	124	205	102	196

* Not possible due to small grain size.

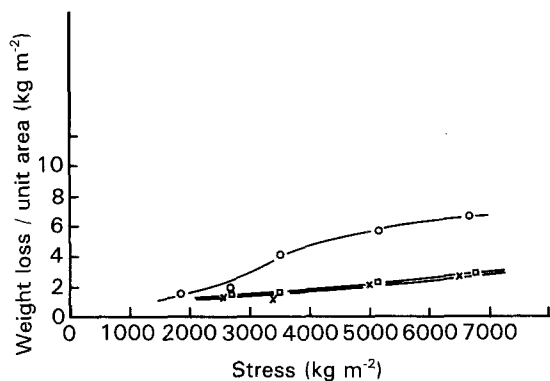


Figure 5 Wear comparison for the extruded alloys at 0.16m s^{-1} sliding speed. \circ , E133; \square , SIB; \times , 326.

It is well known that wear of materials increases with the sliding speed. To clarify the distinction in wear behaviour of these alloys, wear tests on extruded alloys were carried out at relatively higher sliding speeds. The comparison of wear behaviour at the sliding speed of 0.41m s^{-1} is shown in Fig. 6. The wear of alloy E133 was 3–4 times greater than that of alloys 326 and SIB.

The wear curves for the annealed alloys are shown in Fig. 7. In the annealed condition, alloy 326 showed the lowest wear. Slightly higher wear was shown by alloy SIB as compared to alloy 326. The wear of alloy E133 was as large, as was the case in the previous two comparisons.

3.3.3. Friction results

One of the curves recorded to determine the friction force for the extruded alloys is shown in Fig. 8. An almost constant value of friction force was seen for alloy 326, which was recorded for 15 min. A completely different behaviour was observed for alloy E133, which showed large, sharp fluctuations in the friction force plot, although the average value of the friction force was smaller than that of alloy 326. An intermediate behaviour was shown by alloy SIB in which fluctuations in the friction force, nearly half the

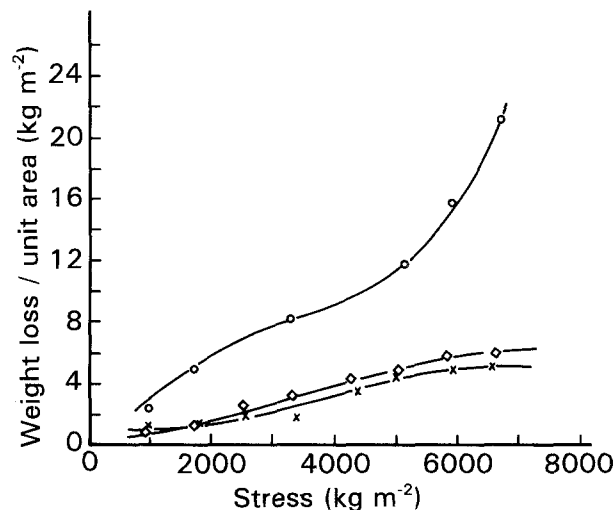


Figure 6 Wear comparison for the extruded alloys at 0.41m s^{-1} sliding speed. \circ , E133; \square , SIB; \times , 326.

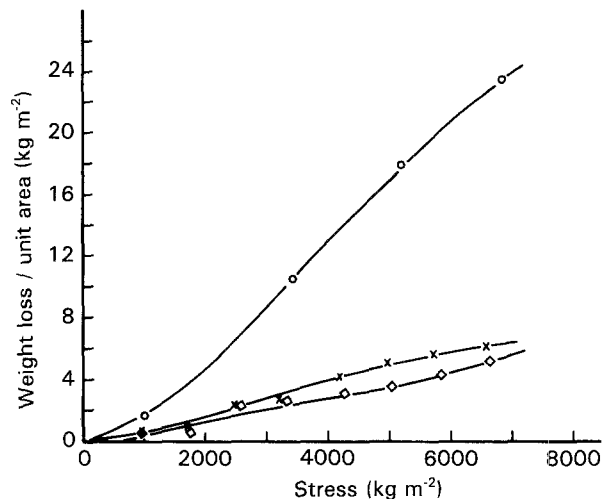


Figure 7 Wear comparison for the annealed alloys at 0.41m s^{-1} sliding speed. \circ , E133; \square , SIB; \times , 326.

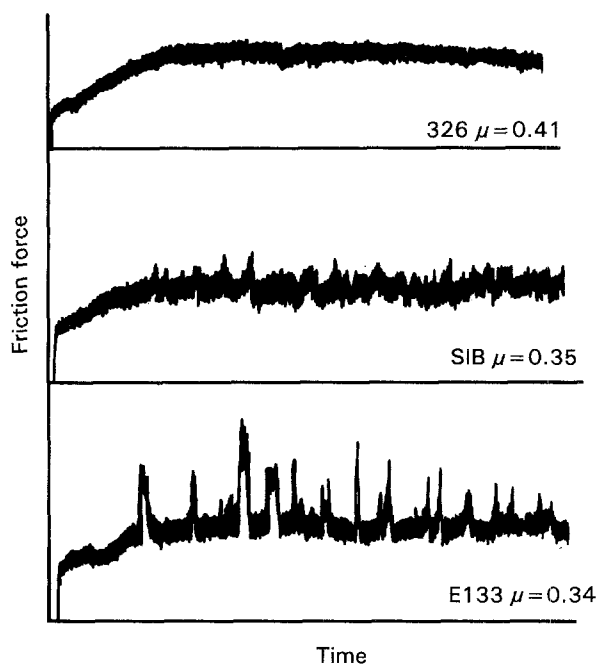


Figure 8 Friction-force plot for the extruded alloys recorded for 15 min.

height of those for alloy E133, could be observed. The average value of coefficients of friction determined for the three extruded alloys 326, SIB and E133 were 0.41, 0.35 and 0.34, respectively.

A further set of curves obtained for the annealed alloys is shown in Fig. 9. The coefficients of friction were slightly decreased for alloys 326 and SIB, but no change was observed in alloy E133. The average value of coefficient of friction for alloy 326 was 0.38, while for the other two alloys it was 0.34. The same degree of fluctuations in friction force for alloys SIB and E133, and almost constant value for alloy 326 (as for the extruded alloys) was observed.

The variation in coefficient of friction as a function of α -phase volume fraction for Cu–41Zn binary alloy is shown in Fig. 10. The friction coefficient was higher when the alloy contained a larger amount of β -phase ($\sim 98\%$). An increase in the α -phase volume fraction

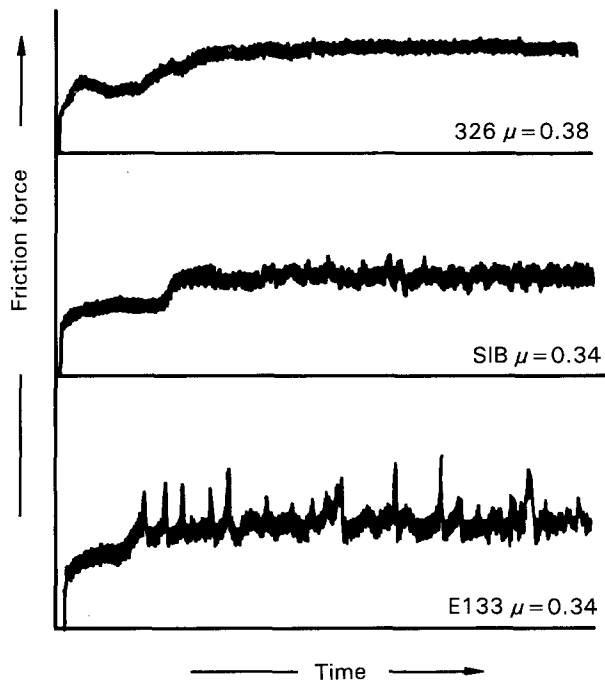


Figure 9 Friction-force plot for the annealed alloys recorded for 15 min.

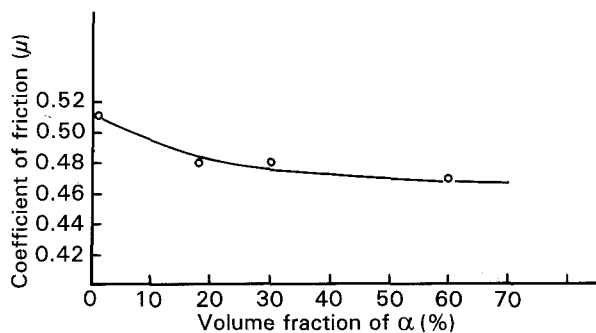


Figure 10 Variation in coefficient of friction as a function of α -phase volume fraction in Cu-41Zn binary alloy.

caused the friction coefficient to decrease. No significant change in friction coefficient was observed when the α -phase volume fraction was increased beyond 40%.

4. Discussion

4.1. Microstructure

The Cu-Zn-Mn and Cu-Zn-Si ternary systems have been studied by several workers [5-7]. The ternary diagrams show that for α or $\alpha + \beta$ brasses, small additions of manganese or silicon go into solid solution and do not form additional phases. In the present investigation, no silicon was detected in either the α or β phases in the three alloys. Hence the solubility of silicon in the α and β -phases must decrease significantly with the addition of manganese. Sun *et al.* [4] studied the microstructure of three Cu-Zn alloys containing manganese and silicon, and they also observed a marked decrease in the solubility of silicon in Cu-Zn system in the presence of manganese. The Cu-Mn-Si ternary section [5] reveals that in the Cu-rich corner the equilibrium microstructure of alloys

containing less than 5 wt% (Mn + Si) consists of a single α -phase at 700 °C. However, the observation of Mn_5Si_3 particles in the α -phase of alloy E133 in the present work, and also by Sun *et al.* [4], indicates that the addition of zinc to the Cu-Mn-Si system must reduce the solubility of both manganese and silicon in the α -phase.

The alloys are extruded in the β -phase region followed by air cooling. The cooling rate depends upon the cross-sectional area of the extruded bars. It is improbable that equilibrium separation of α -phase will have occurred in the extruded products. This is likely to be the reason for the initial increase in the amount of α -phase with temperature in alloys 326 and E133 during annealing (Fig. 4). Low-temperature annealing (20-350 °C) is not sufficient to affect the initial extruded structure. As for the alloy SIB, it had a large cross-sectional area and the cooling rate would have been comparatively slow, not rapid enough to suppress the α separation; hence there was no increase in α -phase volume fraction in this alloy during annealing.

The relative proportions of α and β phases in the alloys were greatly influenced by their aluminium contents. The alloy with high aluminium content (326) contained a high-volume fraction of β -phase, while the alloy with low aluminium content (E133) contained the least amount of β -phase, although the zinc content in the latter alloy was greater than in the former. The alloy with intermediate aluminium content (SIB) had the intermediate volume fraction of β -phase.

Precipitation of α -phase started at much higher temperature (~ 820 °C) in alloy E133 (Fig. 4) than the other two alloys (~ 525 °C). This reflects the presence of aluminium which is a β -stabilizing addition [8]. The α -phase nucleated on either Mn_5Si_3 particles or at β -grain boundaries during quenching and slow cooling.

Varli *et al.* [3] and Sun *et al.* [4] studied the crystallography of manganese silicide (Mn_5Si_3) particles. They found the structure to be hexagonal, with $a = 0.69$ and $c = 0.48$ nm. In the present work Mn_5Si_3 particles were frequently seen in transverse sections (Figs 1a, 2a and 3a) to have hexagonal cross-sections. The shape of these particles is consistent with the crystallography studied in [3, 4]. These authors also suggested that nucleation of Mn_5Si_3 particles occurs in both liquid and solid phases. Particles which form from the liquid are bigger than those which form from the solid solution.

In the present work, the composition of Mn_5Si_3 particles in all three alloys lies in the range 49-52 at% Mn, 39-41 at% Si, and 2-10 at% (Cu + Zn). These values are in agreement with the composition determined by Sun *et al.* [4]. The compositions suggest that copper and zinc atoms probably replace manganese atoms in the lattice rather than silicon atoms.

4.2. Mechanical properties

As mentioned above, the mechanical properties of binary as well as high-tensile brasses are greatly influenced not only by the relative proportions of α - and

β -phases present, but also by alloying additions. The properties of the alloys studied in the present investigation will be discussed on the basis of these facts.

4.2.1. Hardness and microhardness

Comparisons of individual phase hardness for extruded and annealed alloys are shown in Table III. The aluminium content in these alloys not only influenced the relative proportions of the α - and β -phases, but also affected the strength of the phases. The α - and β -phases in the alloy with high aluminium content (326) are much harder than the respective phases in the alloy with lowest aluminium content (E133). The alloy with intermediate aluminium content showed intermediate levels of hardness.

The overall hardness of these brasses would be expected to depend mainly upon the following factors:

(i) relative volume fractions of α - and β -phases present in the alloys;

(ii) grain size of the phases;

(iii) presence of alloying elements, particularly those which are solid-solution strengtheners;

(iv) the presence of residual stresses and cold work.

The extruded 326 alloy was the hardest of the three alloys. This is probably due to the fact that it contained a high β -phase volume fraction, had a small grain size, and contained a relatively large concentration of aluminium which is a solid-solution strengthener. In addition, residual stress could be high due to the small cross-sectional area of the extruded bar. Alloy E133 with the lowest proportion of β -phase and the absence of any solid-solution strengthener, was the softest. Alloy SIB fell between the above two hardnesses.

A decrease in the hardness of all three alloys was observed after annealing (Table II). There are three possible reasons for this decrease: the volume fraction of α -phase may have increased; secondly, annealing results in coarser grain and domain sizes of α - and β -phases, respectively; and thirdly, the heat treatment would recover all the residual stresses which are usually present in extruded materials.

4.2.2. Wear behaviour

Preliminary wear test results showed the dependence of wear of these alloys on the following:

(i) hardness of the alloys;

(ii) relative volume fractions of α - and β -phases present;

(iii) aluminium content of the alloys;

(iv) ease with which hard manganese silicide (Mn_5Si_3) particles become detached from the material during sliding.

As far as the hardness of the alloy is concerned, it has been shown by several investigators [9–12] that wear of materials is, to a certain extent, dependent upon hardness. Hard materials have comparatively high wear resistance, and the results presented here are consistent with this fact. A curve showing the wear as a function of hardness for the three alloys is shown in Fig. 11. Alloys 326 and SIB, which are harder than the

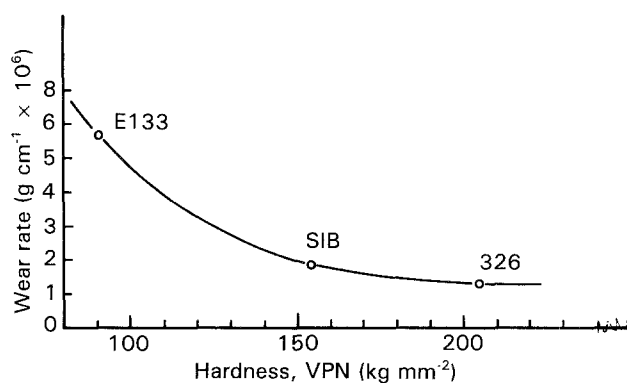


Figure 11 Wear as a function of hardness for the three alloys.

third alloy (E133), showed lower wear. The wear was observed to decrease markedly with the increase in hardness up to about 200 VPN, after which wear seems to decrease very slowly with the further increase in hardness for these alloys.

The higher wear of alloy E133 could be explained on the following basis. Firstly, the alloy contained a high volume fraction of α -phase which is soft and ductile and mainly responsible for the overall low hardness of this alloy. Secondly, the lack of aluminium will maintain the strength of this alloy at a low level. The last and most important factor is the ease of detachment of hard Mn_5Si_3 particles from the low-strength individual matrix phases during sliding. The detachment of these particles is the only reasonable explanation for the large, sharp fluctuations in the friction-force plot shown in Figs 8 and 9. These particles are caught after detachment, for a short time, between the rubbing surfaces. This leads to a three-body abrasive wear situation in which material loss is mainly due to the abrasion. It is clear from the three scanning electron micrographs of the worn surfaces (shown in Fig. 13 below) that abrasion is maximum in alloy E133 and minimum in alloy 326. An intermediate degree of abrasion can be seen for alloy SIB.

It is likely that the factor responsible for the slightly low wear of alloy 326 compared with alloy SIB in the annealed condition is the aluminium content. As discussed earlier, the alloy with high aluminium content (326) is harder than those which contain intermediate and low aluminium contents (SIB and E133, respectively).

In an attempt to identify the role of α - and β -phases in the wear and friction properties, studies were also carried out on a simple binary brass containing 41% Zn. This was heat-treated to vary the volume fraction of the phases. The variation in the wear as a function of α -phase volume fraction is seen in Fig. 12. Slightly higher wear was observed when the alloy contained either relatively large α - or large β -volume fractions. Lowest wear was seen when the structure was composed of β -phase with $\sim 25\%$ of α -phase located mainly at β -grain boundaries.

A possible reason for the wear minimum is that the shocks and vibrations are always present whenever the two metals come into rubbing contact, particularly in dry sliding or in the presence of insufficient (or low quality) lubricants, when stick-slip motion occurs.

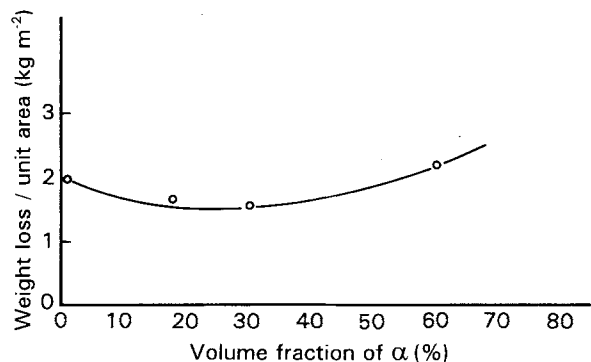


Figure 12 Wear as a function of α -phase volume fraction for Cu-41Zn binary alloy.

This condition leads to a situation of fatigue wear in which subsurface cracks grow due to the continuous loading and unloading of asperities. These subsurface cracks in the β -phase may become blunted when they reach the ductile α -phase, which reduces the amount of fatigue wear.

4.2.3. Coefficient of friction

The average value of friction coefficients for these alloys lies in the range 0.36 ± 0.02 . However, the interesting thing to note is the difference in the friction force behaviour. A fairly uniform friction-force plot was recorded for alloy 326, while large, sharp fluctuations can be seen for alloy E133 (Figs 8 and 9). This difference provides proof of high abrasion in alloy E133 caused by the hard Mn_5Si_3 particles after detachment from the parent metal. These particles, when pulled out during sliding, not only abrade the material but also cause fluctuations in the friction force. Alloy SIB showed an intermediate between the above two behaviours.

The value of friction coefficient in Cu-41Zn alloy seems to depend upon the relative proportions of α - and β -phases present (Fig. 10). The decrease in friction coefficient was significant when α proportion increased from 2% to about 40%, after which it showed an almost constant value. The possible reason for the decrease is that soft and ductile α -phase deforms much more quickly than β . When sufficient α ($\geq 40\%$) is present in the structure, it results in a smearing of the α all over the rubbing contact. This situation leads to α -to- α contact rather than α -to- β or β -to- β contacts. This results in a decrease in the coefficient of friction.

This explanation is in agreement with the study of Taga *et al.* [13] in which they observed a sharp increase in friction coefficient with increasing amount of β -phase.

4.3. Scanning electron microscopy of worn surfaces

Worn surfaces of the alloys were studied in the SEM (Fig. 13). The micrographs show that in alloy 326, the material loss was mainly due to the adhesive and less to abrasive wear, while reverse was the case of alloy

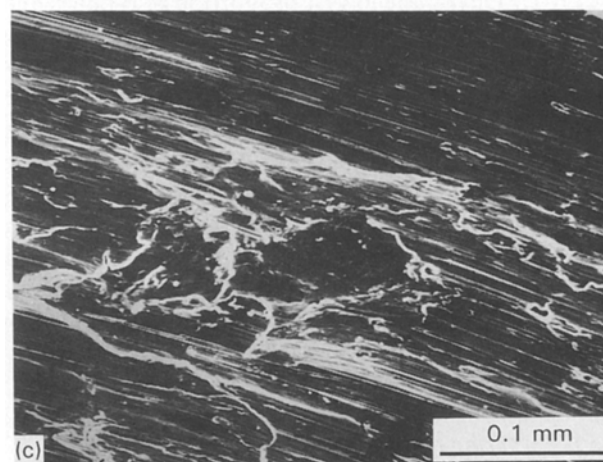
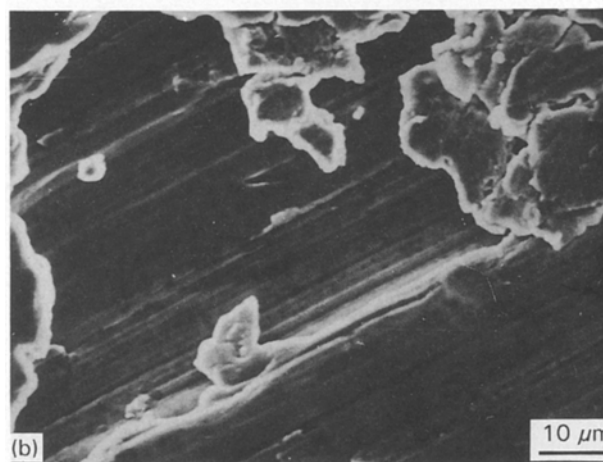
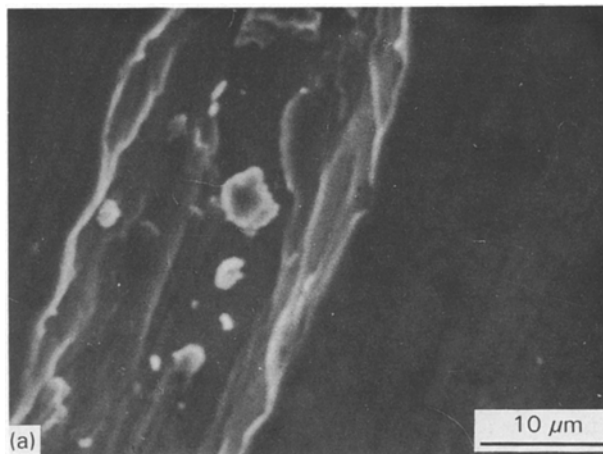


Figure 13 Scanning electron micrographs of the worn surfaces: (a) 326, (b) SIB, (c) E133.

E133 which showed the highest abrasion combined with some adhesive wear. The wear behaviour of alloy SIB was similar to that of alloy 326 but with slightly higher abrasion. The possible reason for less abrasion in alloy 326 is its comparatively high strength and hardness.

5. Conclusions

Three commercial alloys with additions of manganese and silicon were studied for their wear and friction behaviour. The alloys did not show much difference in their friction coefficients, but their wear was found to

be influenced by the following factors:

(i) relative proportions of the α - and β -phases present in the alloy;

(ii) presence of aluminium, which is a solid solution strengthener for Cu–Zn alloys;

(iii) overall hardness of the alloys;

(iv) ease with which Mn_5Si_3 particles become detached from the parent material during sliding.

There was no direct relationship observed in wear and friction behaviour of these alloys. Both the wear and the friction coefficient of the binary Cu–41Zn alloy were found to be functions of the relative phase proportions of the alloy.

Acknowledgements

The authors are grateful to Mckechnic Metals Ltd, Walsall, UK, for the supply of materials. Thanks are also due to Professor G. W. Lorimer and Dr F. D. Bell for many helpful discussions.

References

1. ANON, "Source Book on Copper and Copper Alloys" (ASM, Metals Park, Ohio, 1979) p. 29.

2. ANON, "High Tensile Brasses" CDA Publication No. 42 (Copper Development Association, Potters Bar, UK, 1986) p. 35.
3. K. A. VARLI, N. V. EDNERAL, A. I. LEIKIN, Y. A. SKAKOV and B. V. TYURIN, *Metalloved. Term. Obrab. Met.* **6** (1978) 34.
4. Y. S. SUN, G. W. LORIMER and N. RIDLEY, *Met. Trans.* **20A** (1989) 1199.
5. Y. A. CHANG, J. P. NEWMAN, A. MIKULA and D. GOLDBERG, "Phase Diagrams and Thermodynamic Properties of Ternary Copper Metal Systems", (International Copper Research Association, NSRDS, USA, 1979) p. 543.
6. H. WATANABE, N. KONO and M. GONDA, *J. Jpn Inst. Metals* **36** (1972) 297.
7. H. POPS, *Trans. Metall. Soc. AIME* **230** (1964) 813.
8. C. E. ROLLASON, "Metallurgy for Engineers" (Edward Arnold, 1980) p. 310.
9. R. HOLM, "Mechanical Wear" (American Society for Metals, Ohio, 1950).
10. J. T. BURWELL and C. D. STRANG, *J. Appl. Phys.* **23** (1952) 18.
11. J. F. ARCHARD, *ibid.* **24** (1953) 981.
12. J. F. ARCHARD and E. HURST, *Proc. Roy. Soc.* **236A** (1956) 397.
13. Y. TAGA and K. NAKAGIMA, *Wear* **37** (1976) 356.

Received 13 August

and accepted 14 September 1993